Desalination and Water Treatment
www.deswater.com
doi: 10.1080/19443994.2015.1088804

57 (2016) 18028–18037
August

Taylor & Francis
Taylor & Francis Group

Fe^{3+}/H_2O_2 Fenton degradation of wastewater containing dye under UV irradiation

Hang Xu[a,*], Tianlong Yu[a], Xiaoxi Guo[a], Jianxu Wang[b]

[a]*Chemical Engineering and Pharmaceutics School, Henan University of Science and Technology, Luoyang 471023, China, Tel. +86 379 64231914; emails: xhinbj@126.com (H. Xu), ytl695140552@126.com (T. Yu), jessy.guo@163.com (X. Guo)*
[b]*College of Chemistry and Chemical Engineering, Xinyang Normal University, Xinyang 464000, China, Tel. +86 376 6393882; email: 165389219@qq.com*

Received 22 December 2014; Accepted 20 August 2015

ABSTRACT

We analyzed the photocatalytic effect of ultraviolet on Fe^{3+}/H_2O_2 Fenton degradation of simulated printing sewage containing Reactive Red 6B. Online spectrometry was picked for monitoring to provide more accurate data which is invariably erred by complicated alkali termination in more conventional methods. The photocatalytic effect of ultraviolet on the Fe^{3+}/H_2O_2 Fenton process was assessed by the coefficients of UV promoting effect and reagent utilization under different conditions (Fe^{3+} concentration, H_2O_2 concentration, and pH value). Removal efficiency reached 100% at the optimal condition: 50×10^{-5} mol/L Fe^{3+}, 1×10^{-2} mol/L H_2O_2, and pH 4. Finally, a possible degradation pathway of Reactive Red 6B was proposed.

Keywords: Ultraviolet photocatalytic; Fe^{3+}/H_2O_2 Fenton; Online spectrometry; UV promoting Coefficient; Degradation path

1. Introduction

Sewage from modern industries such as textiles, electroplating or paper production increasingly threatens natural aqueous environments and pollutes drinking water. In recent years, advanced oxidation processes (AOPs) have received increasing attention for their excellent performance in wastewater treatment [1,2]. The Fenton (Fe^{2+}/H_2O_2) process, as an AOPs, possesses substantial active radicals and can achieve oxidation potentials as high as 2.8 eV [3] capable of degrading most contaminants in aqueous solution. Therefore, the Fenton process is outstanding from both an academic and practical research perspective [4,5].

In some research, Fe^{3+} instead of Fe^{2+} expressed a great activity for treating organic contamination [6–8]. Ferric salt is cheaper and more stable than the ferrous equivalent, giving the Fe^{3+}/H_2O_2 system an economic advantage [9,10]. UV catalysis has been studied extensively in conjunction with the Fenton process [11]; however, the specific mechanism was not clear especially at low reagent dosage. Some studies have indicated that UV catalysis is ineffective at high reagent dose limiting its applicability; therefore, we adopted the coefficients of UV promotion and reagent utilization which are characterized as $(k_{UV} - k_d)/k_d$, $(k_{high} - k_{low})/k_{low}$, respectively, to assess degradation efficiency at different reagent concentrations [12].

*Corresponding author.

Online monitoring technology is an advanced, accurate and successive spectrometric method for degradation analysis [13]. Compared to conventional methods that terminate the reaction with chemical reagent of high concentration, online spectrometry minimized experimental error as it involved less manual operation. In this study, absorbance was measured at 523 nm every second to provide instantaneous data on the Fe^{3+}/H_2O_2 process.

2. Methods

2.1. Online spectrometric device

As Fig. 1 depicts, the online detecting device comprises three parts, namely, a transmitter, a reactor, and a recorder. The reactor is composed of a reaction bath which is a characteristic container surrounded by a hollow glass cover and a thermostatic water-circulating bath (Shanghai instrument manufacturer), which provides heat for temperature control. Traditional magnetic stirring was replaced by an electronic stirrer (JJ-1 Tianjin chemical equipment limited company). Last, a UV apparatus provides irradiation and a cycle peristaltic pump (HL-1D, Shanghai instrument manufacturer) drives liquid flow in the overall system through a plastic pipe and micro-scale flowing cuvette (1 ml). The pH of each wastewater sample was adjusted by digital pH meter (PHS-3C-01 experimental pH meter, Shanghai instrument manufacturer). The recorder consisted of a UV–vis spectrometer (SP-756PC Shanghai spectrometric instrument company) attached to a computer (Lenovo laptop Y450). Generally, data were detected by the spectrometer and presented by computer, before processing for removal or kinetic analysis.

2.2. Reagents

Reactive Red 6B (RR6B), which is widely applied in the printing industry, was purchased from Tianjin chemical limited (China). The nitrogen double bond and benzene rings in RR6B contribute to its chemical stability [3,4]. Ferric trichloride, hydrogen peroxide, hydrochloric acid, and sodium hydroxide were also analytical grade.

2.3. GC-MS analysis

Organic substance in sample should be extracted by dichloromethane before GC-MS testing and organic phase was measured. The chromatographic analysis was performed in a Finnigan Trace GC 2000 chromatograph, performing the separation on a DB-5 MS fused quartz capillary chromatographic column (J&W Scientific, Folsom, CA, USA) of 30 m × 0.25 mm i.d. and 0.25 μm phase thickness. The analytes were analysed by mass spectrometry, using a Trace MS 2000 mass spectrometer (Thermo-Quest, Finnigan, USA) working in EI+ mode, coupled to the chromatograph. The working conditions were as follows. The injector

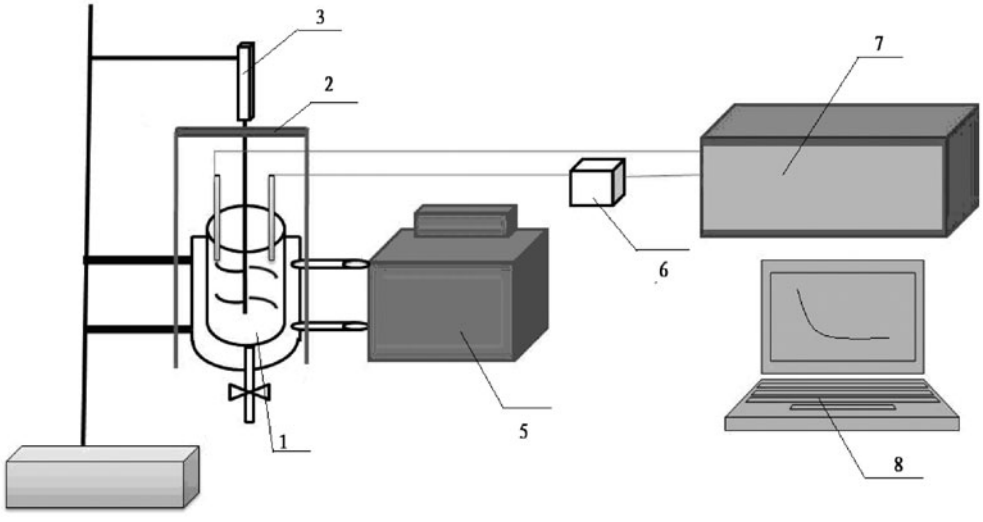

Fig. 1. Online spectrophotometric monitoring system.
Notes: (1) Reactor, (2) UV Light, (3) Electronic stirrer, (4) Thermostatic water-circulator bath, (5) Peristaltic pump, (6) UV spectrophotometer, and (7) PC.

temperature was 250℃. The initial temperature of the oven-heating program was 100℃ for 5 min; the temperature was then raised to 280℃ at 30℃ pre min. The temperatures of the interface and of the ion source were 250 and 150℃, respectively. The carrier gas was helium at a flow of 1 mL/min in constant-flow mode. For the acquisition and processing of the spectrometric data, the Xcalibur software (Thermo Scientific, version 1.4) was used. Sample components derived from RR 6B degradation process were verified by comparison of the mass spectral libraries of the National Institute of Standards and Technology and the Wiley Registry of Mass Spectra Data.

2.4. Main procedure

Prior to the start of the reaction, the online device was initiated to ensure all the reaction data were recorded and the reactive red dyestuff can be dissolved gradually. Ferric ions and hydrogen peroxide were added into the system in sequence, and hydrogen peroxide was added last to avoid experimental error as the source of active radicals. In the experiment, the absorbance at 523 nm (A_{523}) was recorded each second as there is an absorption peak at 523 nm, which is barely influenced by other reagents and was converted to corresponding concentration (C) based on the standard curve equation: $A = 0.03438C + 3.12 \times 10^{-4}$, $R^2 = 0.9999$ (Fig. 2). Although the detection interval is one second, a set point at every 25 s was selected to illustrate the degradation process more clearly.

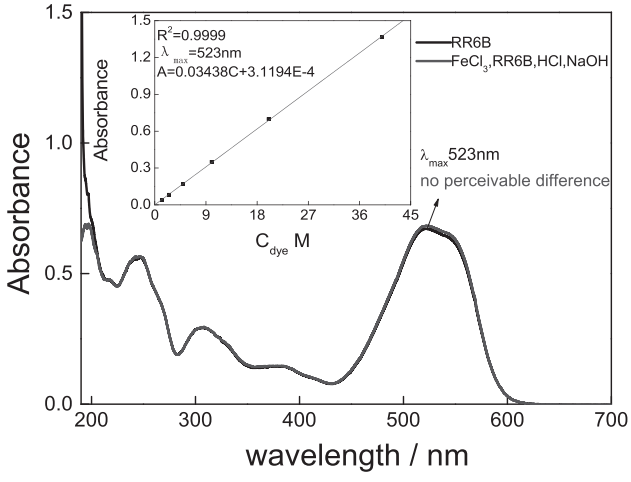

Fig. 2. The standard curve of Reactive Red 6B and exclusion of interference.

3. Result and discussion

3.1. The mechanism of Fe^{3+}/H_2O_2 Fenton process and the UV catalytic effect

The homogenous Fenton process characterized by Fe^{3+}/H_2O_2 is a more practical Fenton system which has been studied extensively. Other than the traditional constituents of the Fenton process, further additives such as ultrasound, ultraviolet, electricity, and heterogeneous nano-Fe_2O_3 or nano-Fe_3O_4 have been introduced to enhance the process [14–17]. In this study, the effect of UV catalysis on Fe^{3+}/H_2O_2 Fenton degradation of RR6B was investigated.

Fe^{3+}, instead of ferrous salt, was selected to avoid oxidation. In brief, H_2O_2 is the main source of reactive radicals which are generated from redox reactions (Eqs. (1) and (2)).

$$H_2O_2 + Fe^{3+} \rightarrow Fe^{2+} + H^+ + {\cdot}O_2H \quad (1)$$

$$H_2O_2 + Fe^{2+} \rightarrow Fe^{3+} + {\cdot}OH + OH^- \quad (2)$$

Hydroxyl radicals possess a high oxidizing potential of 2.8 eV, capable of degrading most contaminants both natural and artificial [3]. However, the radical is easily scavenged by Fe^{2+}, H_2O_2, or by-products such as hydrogen ions and hydroperoxyl radical [18]. The side reactions in the Fe^{3+}/H_2O_2 Fenton process are as follows (Eqs. (3)–(6)):

$$Fe^{2+} + {\cdot}OH \rightarrow Fe^{3+} + OH^- \quad (3)$$

$$H_2O_2 + {\cdot}OH \rightarrow {\cdot}O_2H + H_2O \quad (4)$$

$${\cdot}O_2H + {\cdot}OH \rightarrow H_2O + O_2 \quad (5)$$

$$H^+ + e^- + {\cdot}OH \rightarrow H_2O \quad (6)$$

Meanwhile, although Fenton reagents can contribute to high degradation efficiency, this could be decreased with excessive Fe^{3+} or H_2O_2 or if the pH remains too low. So the relation between Fenton constituents and removal rate needs to be investigated to attain high degradation efficiency.

It has been verified in numerous studies that UV light has certain synergetic effects on the Fenton process [19]. The widely accepted mechanism is that UV light accelerates charge transfer from Fe^{3+} to Fe^{2+}, thus more Fe^{2+} is generated to react with H_2O_2 and produce hydroxyl radicals. Additionally, some radicals are produced by photolysis of H_2O_2 under UV irritation. Alternatively, the photocatalytic enhancement of

treatment efficiency could be ascribed to photo-induced oxidation by inner-sphere electron-transfer reaction of some intermediates or organic substrates [12].

3.2. The degraded percentage of RR6B at different conditions

The removal efficiency of RR6B is defined as $[RR6B]_0 - [RR6B]_i/[RR6B]_0$, where $[RR6B]_0$ represents the initial concentration of RR6B and $[RR6B]_i$ stands for the instant concentration of Reactive Red 6B at time *i*.

3.2.1. Effect of initial Fe^{3+} dosage

Fe^{3+} acts as not only a reagent but also as a catalyst in the basic redox Fenton reactions as Eqs. (1)–(3) show. The ferric ions reacted with hydrogen peroxide to yield ferrous ions and perhydroxyl radicals. The ferrous ions catalyze the conversion of hydrogen peroxides to hydroxyl radicals for contaminant degradation, and meanwhile, the ferrous ions will revert to ferric ions after losing an electron. Fig. 3 reveals that the highest removal efficiency (99%) was achieved when the concentration of Fe^{3+} was 50×10^{-5} mol/L. Generally, regardless of light condition (dark or UV), the degradation efficiency increases when the concentration of Fe^{3+} goes up. However, when the concentration rose to 200×10^{-5} and 300×10^{-5} mol/L, the efficiency of degradation stalled and fell which can be explained by excessive iron ions scavenging radicals (Eq. (3)). Another observed phenomenon was that UV catalysis was more effective with low Fe^{3+} concentration, causing an improvement of about 50% at 1.5×10^{-5} mol/L Fe^{3+}. However, in most cases, while UV accelerated degradation, it did not improve the total removal. Therefore, the degree of degradation promotion by UV should be quantized.

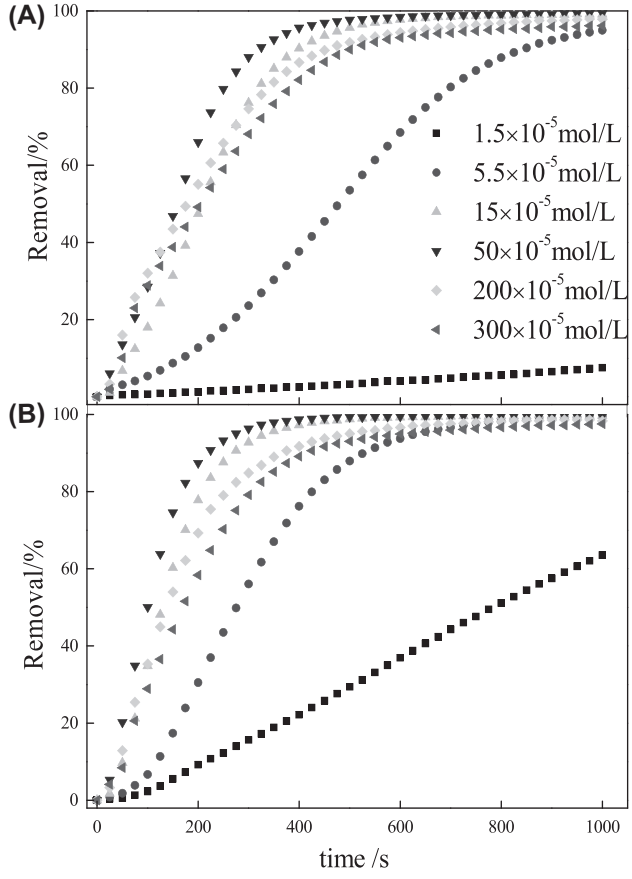

Fig. 3. The effect of Fe^{3+} concentration (A) in the dark, (B) under UV irradiation. Experimental conditions: $[RR6B]_0$: 4×10^{-5} mol/L $[H_2O_2]_0$: 2.5×10^{-3} mol/L pH 3.15 T = 15°C UV Intensity (Distance = 1 m) = 62–69 μW/cm^2.

3.2.2. Effect of initial H_2O_2 dosage

H_2O_2 is another important component of the Fenton reaction. It can be concluded from Fig. 4 that the Fe^{3+}/H_2O_2 process was effective in the selected H_2O_2 dosage range, and removal reached almost 60% at 1.56×10^{-5} mol/L H_2O_2. But it was most efficient at 1×10^{-2} mol/L H_2O_2 both in the dark and under UV irradiation. At this H_2O_2 dosage, the removal reached almost 90% after 200 s; however, this time was reduced under UV irradiation. Similarly to the effect of iron ions, removal efficiency is improved with increasing concentrations of H_2O_2 from 1.56×10^{-5} to 1×10^{-2} mol/L. But a downward trend appeared when the concentration was 2×10^{-2} mol/L and this trend became more obvious at 5×10^{-2} mol/L, with excessive H_2O_2 the intermediate perhydroxyl radicals would mainly serve as hydrogen radical scavengers leading to a reduction in degradation as shown by Eqs. (4) and (5). The Fig. 4(B) can be explained by UV catalyzing the reaction by accelerating the electron transfer and improving the utilization of H_2O_2. Meanwhile, UV catalyzes H_2O_2 decomposition and generation of radicals to enhance degradation. What is remarkable is that under UV irradiation removal was increased 30% at a small concentration of 1.56×10^{-5} mol/L when compared to dark condition.

3.2.3. Effect of initial pH

It has been proved that the homogenous Fenton process works under meta-acid conditions [3,4], and previous studies showed that the favorable pH values for Fenton-like processes range from 3.0 to 4.0

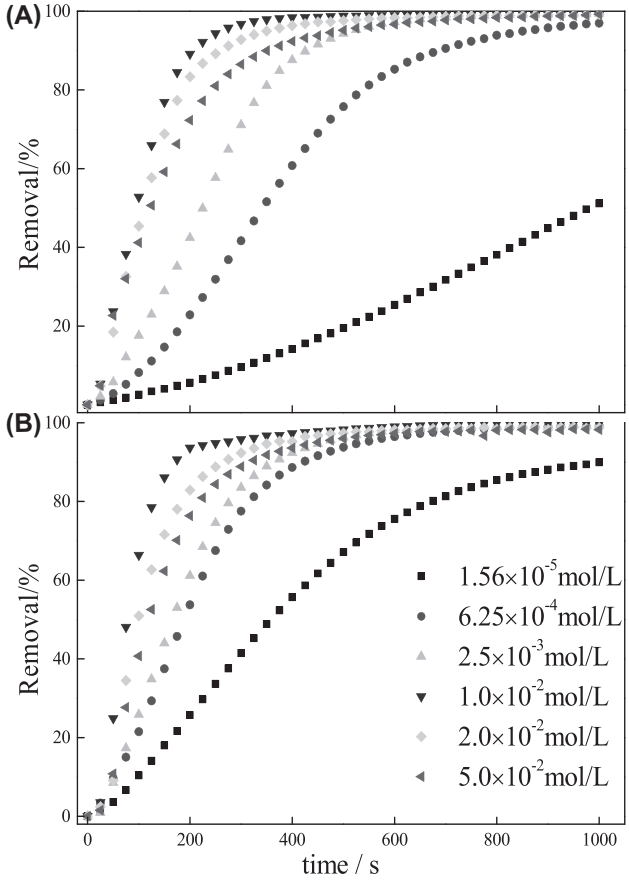

Fig. 4. The effect of H_2O_2 concentration (A) in the dark, (B) under the UV irradiation. Experimental conditions: $[RR6B]_0$: 4×10^{-5} mol/L $[Fe^{3+}]_0$: 50×10^{-5} mol/L pH 3.15 T = 15℃ UV Intensity (Distance = 1 m) = 62–69 μW/cm^2.

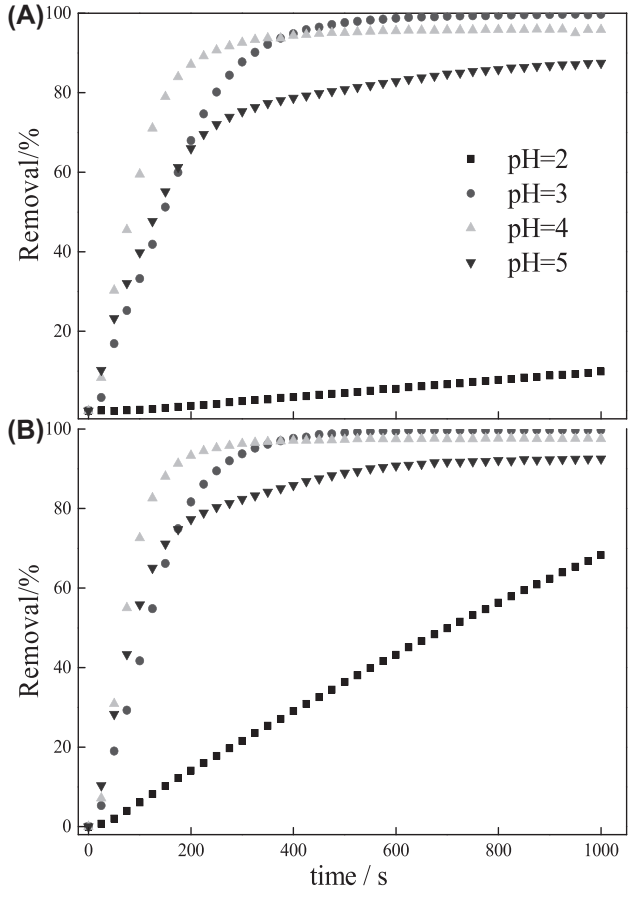

Fig. 5. Effect of pH value (A) in the dark, (B) under the UV irradiation). Experiment conditions: $[RR6B]_0$: 4×10^{-5} mol/L $[Fe^{3+}]_0$: 50×10^{-5} mol/L $[H_2O_2]_0$: 1×10^{-2} mol/L T = 15℃ UV Intensity (Distance = 1 m) = 62–69 μW/cm^2.

[3,13,20]. Fig. 5 shows that the most suitable pH value of Fe^{3+}/H_2O_2 process here was 4.0, which is in accordance with the available literature [4,13]. The Fe^{3+}/H_2O_2 Fenton process barely works at pH of 2 with a final degradation of merely 10% due to the scavenging effect of hydrogen ions. When the same experiment was carried out under UV irradiation, about 60% rise in efficiency was observed as the side effects of hydrogen ions were inhibited and electron transfer accelerated by UV irradiation, enhancing the reaction between Fe^{2+} and H_2O_2. Consequently, more radicals were available for degradation. When the pH value increased to 3, 4, or 5, the removal increased quickly during the initial 300 s and the ultimate removal can reach over 90%. Moreover, at pH 5, the degradation becomes deficient resulting from the decomposition of hydrogen peroxide and the formation of iron hydroxide complexes. In addition, this indicates that the degradation rate of RR6B at pH 4 is optimal. Therefore, pH 4 has been selected as the optimum solution acidy for degradation.

3.3. First-order kinetics analysis

Some research suggests that first-order kinetics fit the Fenton or homologous Fenton processes [12,13]. Here, data were processed by first-order kinetics, and the relevant reaction rate constants are illustrated in Fig. 6. The fitting coefficients of diverse situations are mostly above 0.98 and shown in Table 1. It can be concluded that there is a promotion of removal rate under UV irradiation under different conditions, which is clearly shown in Fig. 6. An unexpected phenomenon here is that UV catalysis was not consistently efficient under different conditions. The UV catalysis at low or medium Fe^{3+} and H_2O_2 dosages as well as low pH values was more efficient than that

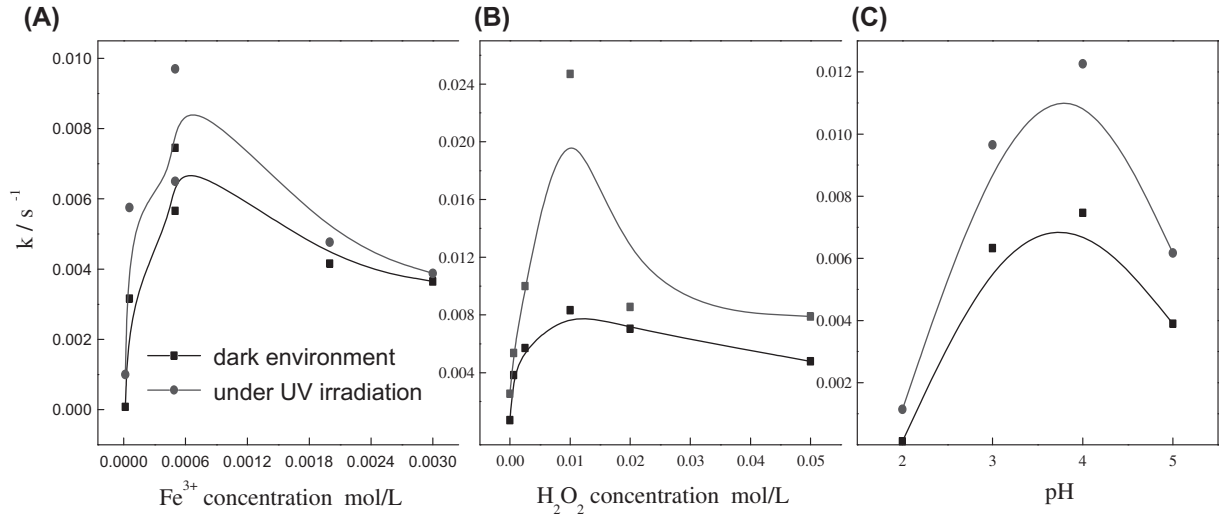

Fig. 6. Apparent rate constant of degradation at different conditions (A) at different Fe^{3+} concentrations, (B) at different H_2O_2 concentration, and (C) at different pH values.

Table 1
First-order kinetics fitting coefficients at different conditions

RR6B (mol/L)	Fe^{3+} (mol/L)	H_2O_2 (mol/L)	pH	T (°C)	R^2	R^2 (UV)
4E-5	1.5E-5	2.5E-3	3.15	15	0.996	0.989
4E-5	5.5E-5	2.5E-3	3.15	15	0.968	0.993
4E-5	15E-5	2.5E-3	3.15	15	0.977	0.964
4E-5	50E-5	2.5E-3	3.15	15	0.990	0.985
4E-5	200E-5	2.5E-3	3.15	15	0.989	0.953
4E-5	300E-5	2.5E-3	3.15	15	0.976	0.952
4E-5	50E-5	1.56E-5	3.15	15	0.976	0.997
4E-5	50E-5	6.25E-4	3.15	15	0.991	0.993
4E-5	50E-5	2.5E-3	3.15	15	0.957	0.990
4E-5	50E-5	1E-2	3.15	15	0.967	0.961
4E-5	50E-5	2E-2	3.15	15	0.973	0.953
4E-5	50E-5	5E-2	3.15	15	0.988	0.964
4E-5	50E-5	1E-2	2	15	0.997	0.994
4E-5	50E-5	1E-2	3	15	0.987	0.997
4E-5	50E-5	1E-2	4	15	0.975	0.982
4E-5	50E-5	1E-2	5	15	0.977	0.973

with high reagent dosages and pH values. It can also be concluded that H_2O_2 is the most influential condition of the Fe^{3+}/H_2O_2 process since the degradation rate at 0.01 mol/L H_2O_2 is 200% higher than that at 50×10^{-5} mol/L Fe^{3+} or pH of 4.

3.4. The coefficient of UV promoting effect and reagent utilization

Based on first-order kinetics fitting, degradation rates differed with conditions. To understand the specific effect of UV catalysis, the coefficient of UV promoting effect was calculated (Eq. (7)):

$$\lambda = \frac{k_{UV} - k_d}{k_d} \tag{7}$$

where k_{UV} is the degradation rate under UV irradiation; k_d is the degradation rate in the dark; λ is the coefficient of UV promoting effect.

From Fig. 7, it is clear that the UV light works more efficiently at low Fe^{3+} and H_2O_2 dosages or low

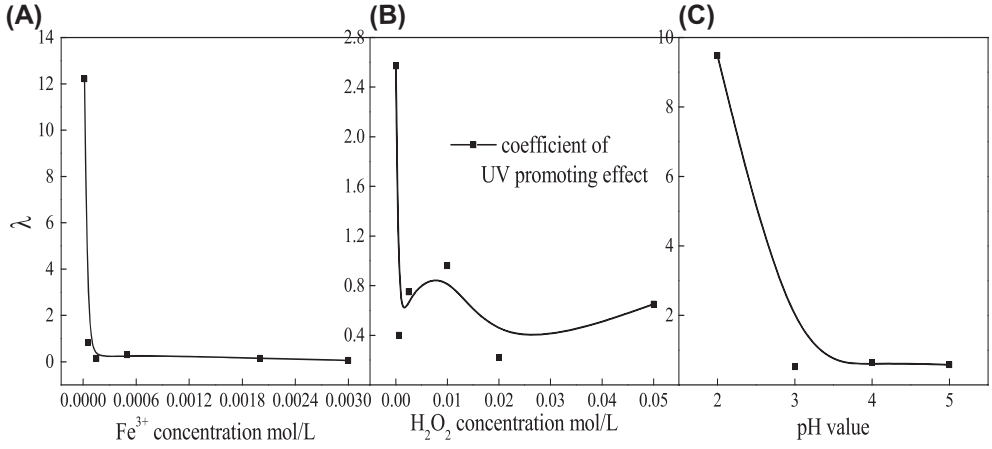

Fig. 7. Coefficient of UV promoting effect at different conditions (A) at different Fe^{3+} concentrations, (B) at different H_2O_2 concentrations, and (C) at different pH values.

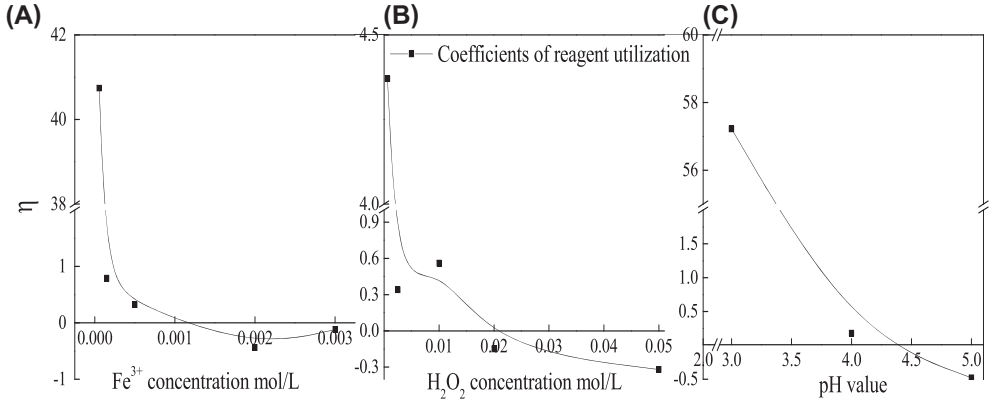

Fig. 8. Coefficients of reagent utilization at different conditions (A) at different Fe^{3+} concentrations, (B) at different H_2O_2 concentrations, and (C) at different pH values.

pH values, while relatively poorly with high dosage or weak acidity. That is, the UV promoting coefficients are 12.2, 2.6, and 9.5 at 1.5×10^{-5} mol/L Fe^{3+}, 1.56×10^{-5} mol/L H_2O_2, and pH 2, respectively. All three parts of Fig. 7 drop sharply and then level out along the horizontal axis, and this tendency can be characterized as a capital letter "*L*." Correspondingly, the UV catalytic effect is weak at high reagent dosage as the Fenton reaction takes place predominantly when the reagent concentration is sufficient and degradation rate is high even without UV irradiation, this indicates that UV catalytic effect is weakened. Hence, the UV should be initiated early to accelerate the degradation while shortening test duration and then turned off later.

Another important indicator is the coefficient of reagent utilization. A similar equation is characterized as Eq. (8):

$$\eta = \frac{k_{high} - k_{low}}{k_{low}} \tag{8}$$

k_{high} is the reaction rate at high reagent dosage; k_{low} is the reaction rate at low reagent dose; η represents the coefficient of reagent utilization.

Fig. 8 illustrates the coefficient of reagent utilization with different Fe^{3+}, H_2O_2 concentrations and various pH values. It is obvious that coefficients drop from positive to negative, theoretically if $\eta \geq 0$, then added reagents have a promoting effect on the

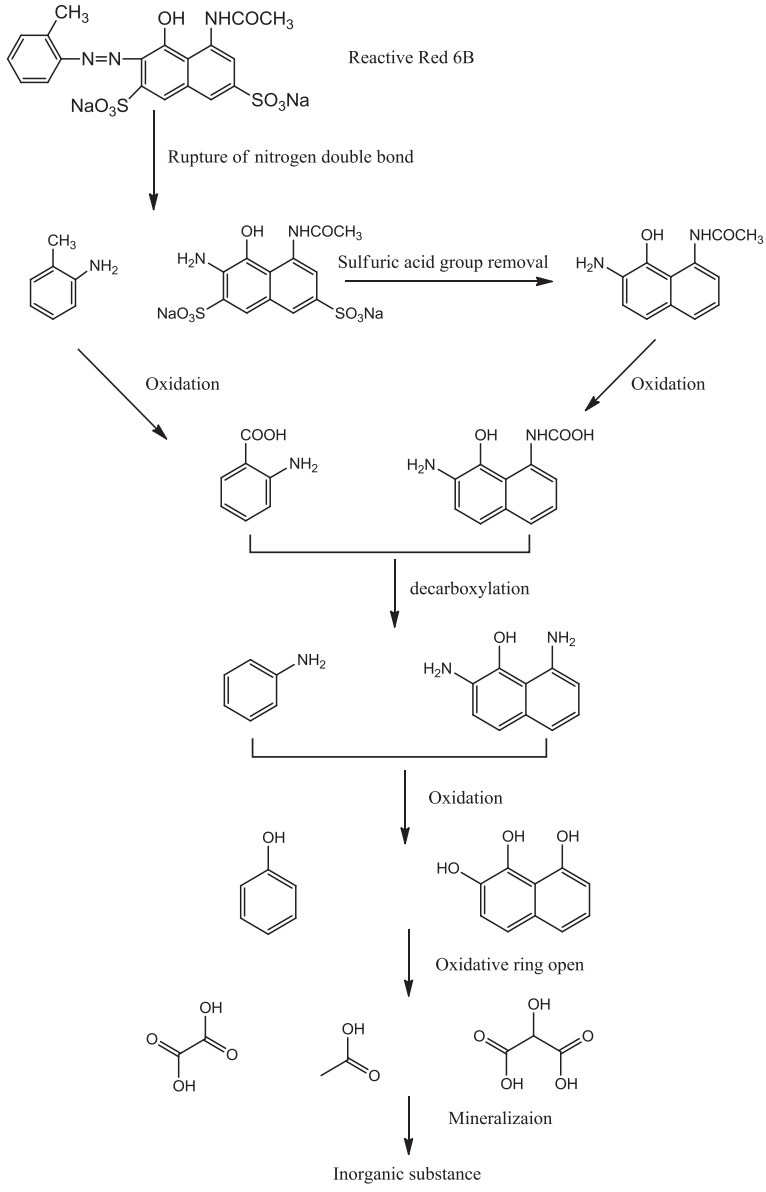

Fig. 9. Degradation path of Reactive Red 6B.

degradation and were made the best use of. On the contrary, $\eta < 0$ indicates that the overdosed reagent does not accelerate the reaction and conversely act as inhibitors. In detail, the coefficient of Fe^{3+} was 41 when the dose of Fe^{3+} increased from 1.5×10^{-5} to 5.5×10^{-5} mol/L and decreased to 0 with the addition of more Fe^{3+}. Finally, the value turned negative when the dose of ferric ion rose above 0.002 mol/L. Similar patterns were found in the studies of H_2O_2 and pH. At the earlier stage of degradation, the coefficient is much larger than that of mid-phase, which turns to a negative value eventually. Therefore, in this study, superior Fe^{3+}/H_2O_2 Fenton process conditions can be determined from Fig. 8 from the perspective of the efficiency of reagents.

3.5. The simple estimation of the Reactive Red 6B degradation path

According to the GC-MS analysis, main by-products of the degradation were hydroxyl malonic, oxalic acid, and acetic. The chemical structure of RR6B and the estimated degradation path are shown in Fig. 9. According to other studies regarding azo dye degradation, the first step is the cleavage of a nitrogen double bond resulting in naphthalene- and

benzene-based compounds. These intermediates can both be further degraded to aliphatic compounds. Finally, all these by-products will be mineralized to lower weight molecules or inorganic substances [12,13,15,21].

4. Conclusions

The Fe^{3+}/ H_2O_2 Fenton degradation of simulated dyeing wastewater with RR6B under UV irradiation was investigated with online spectrometry. The process obeys first-order kinetics with most fitting coefficients above 0.98 and removal efficiency reached 100% at the optimal conditions: 50×10^{-5} mol/L Fe^{3+}, 1×10^{-2} mol/L H_2O_2, and pH 4. From a mathematic perspective, the coefficients of UV promoting effect and reagent utilization were selected to evaluate the UV catalytic effect and study the relationship between Fenton reagents and removal rate, respectively. The results show that UV promotion is more efficient with low reagent concentrations and strong acidic conditions than with higher doses and weak acidity. Moreover, the reagent utilization coefficient intuitively describes the relation between reagent dosage and removal rate, that is, increasing reagent concentration up to optimal improves degradation efficiency and the coefficient is positive until excessive reagent turns into radical scavenger when the dosage is above optimal and the coefficient turns negative. Therefore, a high coefficient of UV promoting effect and a positive reagent utilization coefficient are necessary to achieve high degradation efficiency for wide applications. Finally, the degradation path of RR6B was speculated to predict some intermediates and possible final products.

Acknowledgements

This work was supported by the National Nature Science Foundation of China (Number: 21006057) and Henan Provincial Science and Technology Foundation (Numbers: 142300410202, 142102210427 and 122102210551).

References

[1] M. Mehrjouei, S. Müller, D. Möller, Removal of fuel oxygenates from water using advanced oxidation technologies by means of falling film reactor, Chem. Eng. J. 211–212 (2012) 353–359.
[2] M. Vallejo, M.F.S. Román, I. Ortiz, Overview of the PCDD/Fs degradation potential and formation risk in the application of advanced oxidation processes (AOPs) to wastewater treatment, Chemosphere 118 (2015) 44–56.
[3] S. Tunç, T. Gürkan, O. Duman, On-line spectrophotometric method for the determination of optimum operation parameters on the decolorization of Acid Red 66 and Direct Blue 71 from aqueous solution by Fenton process, Chem. Eng. J. 181 (2012) 431–442.
[4] M.A. Behnajady, N. Modirshahla, F. Ghanbary, A kinetic model for the decolorization of C.I. Acid Yellow 23 by Fenton process, J. Hazard. Mater. 148 (2007) 98–102.
[5] R.C. Martins, L.R. Henriques, R.M.Q. Ferreira, Catalytic activity of low cost materials for pollutants abatement by Fenton's process, Chem. Eng. Sci. 100 (2013) 225–233.
[6] H.R. Rajabi, O. Khani, M. Shamsipur, V. Vatanpour, High-performance pure and Fe^{3+}-ion doped ZnS quantum dots as green nanophotocatalysts for the removal of malachite green under UV-light irradiation, J. Hazard. Mater. 250–251 (2013) 370–378.
[7] M. Shamsipur, H.R. Reza Rajabi, O. Khani, Pure and Fe^{3+}-doped ZnS quantum dots as novel and efficient nanophotocatalysts: Synthesis, characterization and use for decolorization of Victoria blue R, Mat. Sci. Semicond. Process. 16 (2013) 1154–1161.
[8] M. Shamsipur, H.R. Rajabi, Study of photocatalytic activity of ZnS quantum dots as efficient nanoparticles for removal of methyl violet: Effect of ferric ion doping, Spectrochim. Acta, Part A 122 (2014) 260–267.
[9] D. Rubio, E. Nebot, J.F. Casanueva, Comparative effect of simulated solar light, UV, UV/H_2O_2 and photo-Fenton treatment (UV-Vis/H_2O_2/$Fe^{2+,3+}$) in the Escherichia coli inactivation in artificial seawater, Water Res. 47 (2013) 6367–6379.
[10] X. Li, T. Shen, D. Wang, Photodegradation of amoxicillin by catalyzed Fe^{3+}/H_2O_2 process, J. Environ. Sci. 24 (2012) 69–275.
[11] I. Grčić, M. Maljković, S. Papić, Low frequency US and UV-A assisted Fenton oxidation of simulated dyehouse wastewater, J. Hazard. Mater. 197 (2011) 272–284.
[12] M.J. Liou, M.C. Lu, J.N. Chen, Oxidation of explosives by Fenton and photo-Fenton processes, Water Res. 37 (2003) 3172–3179.
[13] H. Xu, D. Zhang, W. Xu, Monitoring of decolorization kinetics of Reactive Brilliant Blue X-BR by online spectrophotometric method in Fenton oxidation process, J. Hazard. Mater. 158 (2008) 445–453.
[14] M. Siddique, R. Farooq, G.J. Price, Synergistic effects of combining ultrasound with the Fenton process in the degradation of Reactive Blue 19, Ultrason. Sonochem. 21 (2014) 1206–1212.
[15] H. Kusic, D. Juretic, N. Koprivanac, Photooxidation processes for an azo dye in aqueous media: Modeling of degradation kinetic and ecological parameters evaluation, J. Hazard. Mater. 185 (2011) 1558–1568.
[16] S. Guo, G. Zhang, J. Wang, Photo-Fenton degradation of rhodamine B using Fe_2O_3–Kaolin as heterogeneous catalyst: Characterization, process optimization and mechanism, J. Colloid Interface Sci. 433 (2014) 1–8.
[17] J. He, X. Yang, B. Men, Heterogeneous Fenton oxidation of catechol and 4-chlorocatechol catalyzed by nano-Fe_3O_4: Role of the interface, Chem. Eng. J. 258 (2014) 433–441.

[18] H. Xu, Q. Tang, Y.N. Liu, Degradation kinetics and mechanics of methylene blue by complex ultraviolet and hydrogen peroxide process, Adv. Mater. Res. 356–360 (2011) 1066–1069.
[19] A. Zhang, Y. Li, Removal of phenolic endocrine disrupting compounds from waste activated sludge using UV, H_2O_2, and UV/H_2O_2 oxidation processes: Effects of reaction conditions and sludge matrix, Sci. Total Environ. 493 (2014) 307–323.
[20] N. Masomboon, C. Ratanatamskul, M.C. Lu, Mineralization of 2,6-dimethylaniline by photoelectro-Fenton process, Appl. Catal. A 384 (2010) 128–135.
[21] J.R. Steter, W.R. Barros, M.R. Lanza, Electrochemical and sonoelectrochemical processes applied to amaranth dye degradation, Chemosphere 117 (2014) 200–207.